AEE 325 Lab 02

Zakary Steenhoek | 1224635594 | Section 14118

Procedure: Wednesday, February 5th, 2025 @ 6:00pm

Report: Wednesday, February 19th, 2025

I. Abstract

This experiment aimed to investigate the bending behavior of Aluminum 7075 cantilever beams under applied loads and validate beam bending theory using strain gage measurements. Three different beam configurations were tested: (1) a uniform cross-section beam with two strain gages, (2) a uniform cross-section beam with three strain gages, and (3) a beam with a linearly varying cross-section. The applied load and strain data were recorded to determine Young's modulus EEE and Poisson's ratio v\nuv for the material and to analyze the stress distribution along the beam length. Experimental results were compared with theoretical predictions based on bending moment equations. Deviations between the measured and theoretical values were examined, and possible sources of error were discussed. The findings contribute to a deeper understanding of stress and strain variation in cantilever beams with different geometries.

II. Objectives | Procedure

The primary objective of this experiment was to analyze the bending behavior of Aluminum 7075 cantilever beams under applied loads and validate theoretical predictions. The experiment aimed to determine the Young's modulus E and Poisson's ratio v of the material and examine how stress distribution varies along beams with different configurations. The effects of a variable cross-section on stress and strain were investigated to assess the accuracy of beam bending theory in predicting the behavior of geometrically varying structures. The relevant equations are seen below, Eq. [1] and Eq. [2]:

$$\sigma_{axial} = \frac{M(x) \cdot y_{max}}{I(x)} \quad [1]$$

$$\sigma_{axial} = E \cdot \epsilon_{axial} \quad [2]$$

The experiment was conducted using a testing setup with cantilevered beams instrumented with strain gages at specific locations. Three different beam configurations were tested to assess distinct aspects of bending behavior. First, a uniform cross-section beam with two strain gages - one on the top surface and one on the bottom - was analyzed to measure axial and lateral strains at the outer fibers. This data was used to compute material properties, specifically Young's modulus and Poisson's ratio. Second, a uniform cross-section beam with three strain gages placed at different locations along the length was tested to evaluate the variation of stress as a function of bending moment. Finally, a variable cross-section beam, designed to maintain constant stress along its length, was instrumented with four strain gages to examine how changes in cross-section geometry influence strain and stress distribution.

For each beam configuration, loads were applied incrementally in the elastic range, and strain readings were recorded at each stage. Multiple measurements of beam geometry and strain gage locations were averaged to ensure accuracy in calculations. Data collected from the strain gages was used to compute stress distributions, compare experimental results with theoretical predictions, and discuss uncertainty and error due to things such as strain gage placement, material inconsistencies, measurement uncertainties, and analytical uncertainty.

III. Results | Evaluation | Discussion

The shear force and moment diagrams for the constant cross-section beam:

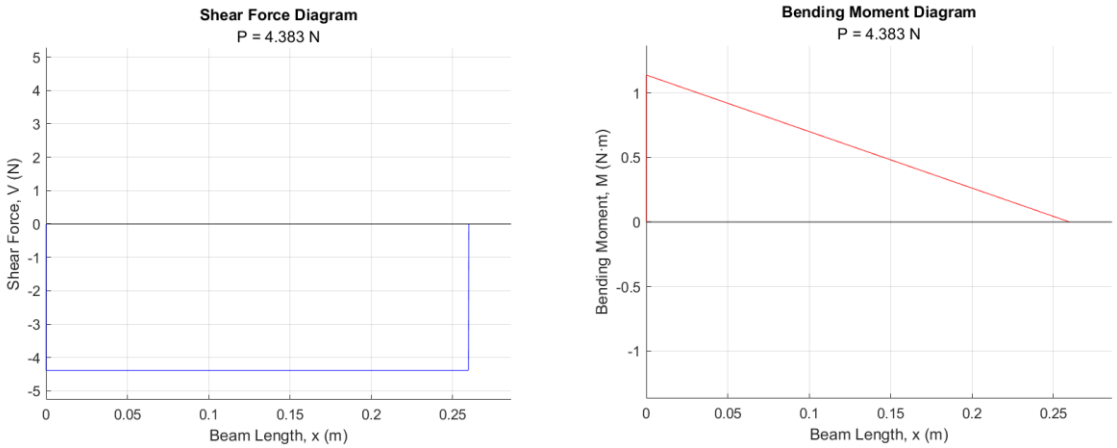

Figure 1 & 2: Shear force and bending moment diagrams for the constant cross-section beam, cantilevered at one end and loaded with a force $P = 4.383\,N$.

The Youngs Modulus estimated from the slope of the load-strain diagram was found to be $E = 64.015\,GPa$. This compares well to published material data about 7075 aerospace aluminum, for which Young's modulus is found to be $E \approx 70\,GPa$[1][2].

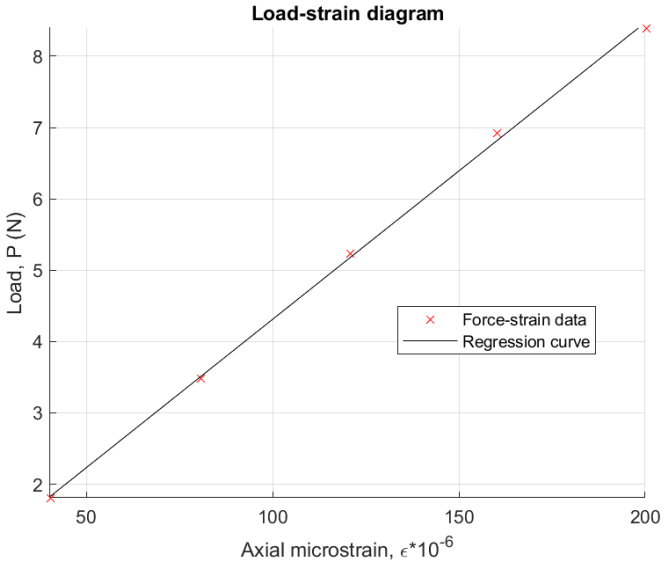

Figure 3: Load-strain diagram for 7075 aluminum.

Poisson's Ratio, estimated from the slope of the strain-strain diagram, is found to be $v = 0.3242$. Published data finds Poisson's Ratio to be $v \approx 0.32$[1][2].

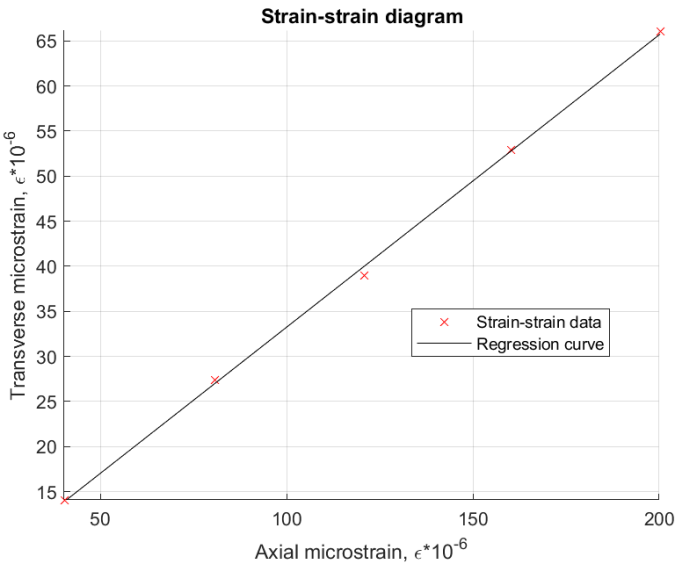

Figure 4: Strain-strain diagram for 7075 aluminum

For the constant cross-section, variable stress beam, theoretical and experimental stresses were computed at each of the 5 load values:

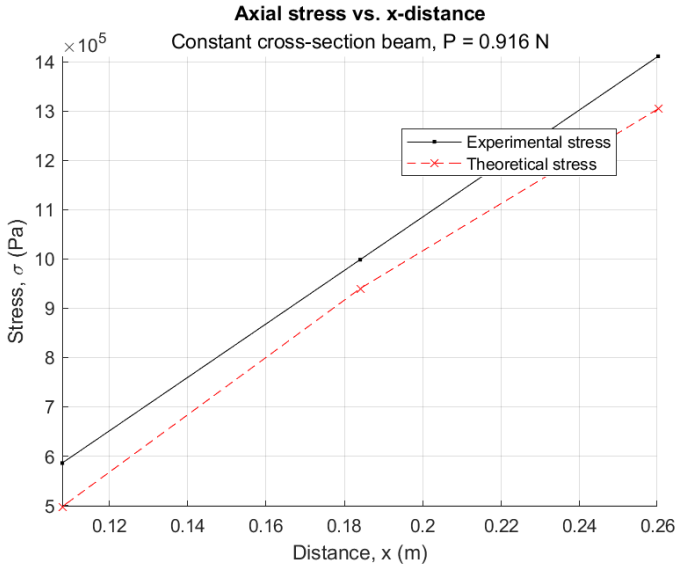

Figure 5: Axial stress over the length of the beam, $P = 0.916\,N$

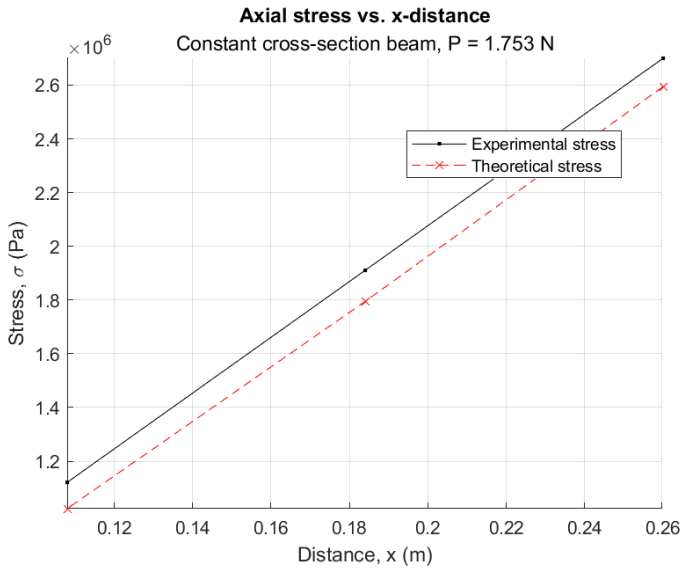

Figure 6: Axial stress over the length of the beam, $P = 1.753\ N$

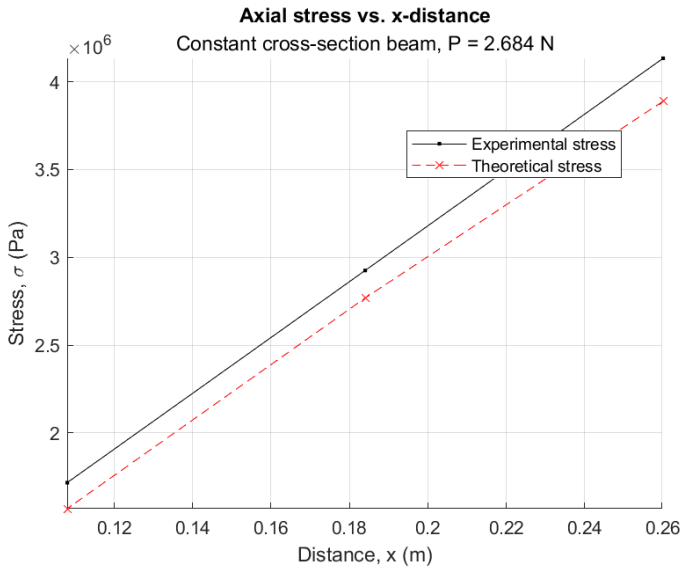

Figure 7: Axial stress over the length of the beam, $P = 2.684\ N$

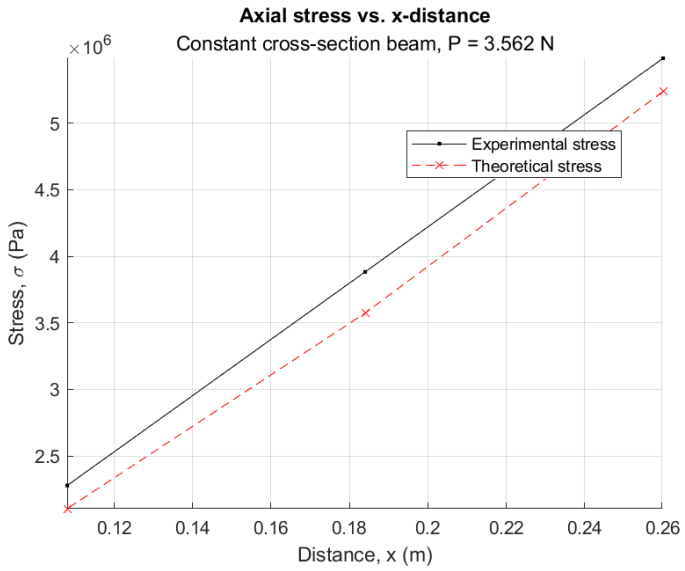

Figure 8: Axial stress over the length of the beam, $P = 3.562\ N$

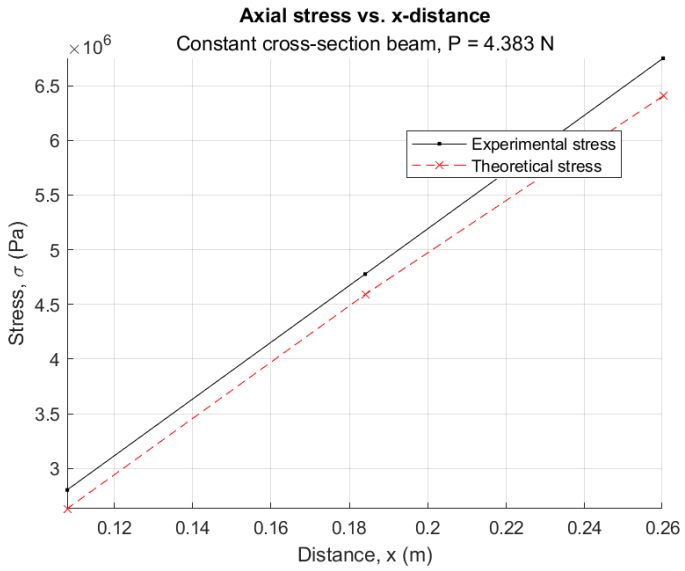

Figure 9: Axial stress over the length of the beam, $P = 4.383\ N$

These plots show that the experimental data collected during the lab does match the analytical results obtained from classroom equations. For each of the load magnitudes, there is little deviation from the expected results, though there is consistently slightly more as the moment arm increases.

For the variable cross-section, constant stress beam, theoretical and experimental stresses were computed at each of the 5 load values:

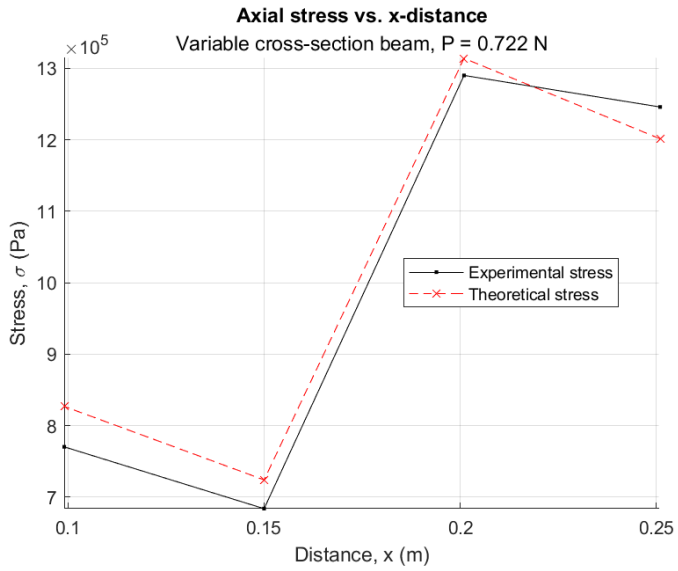

Figure 10: Axial stress over the length of the beam, $P = 0.722\,N$

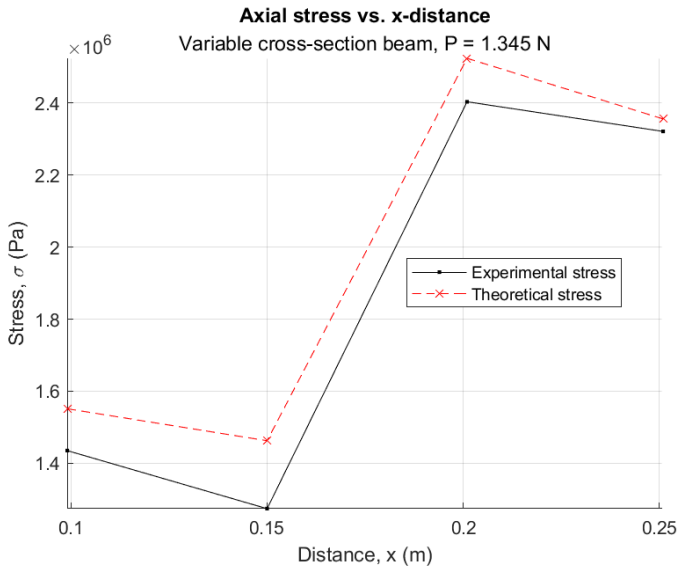

Figure 11: Axial stress over the length of the beam, $P = 1.345\,N$

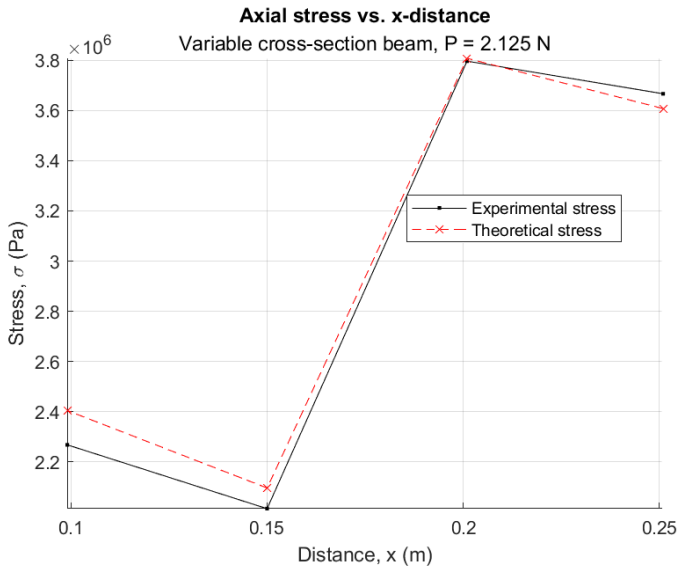

Figure 12: Axial stress over the length of the beam, $P = 2.125\,N$

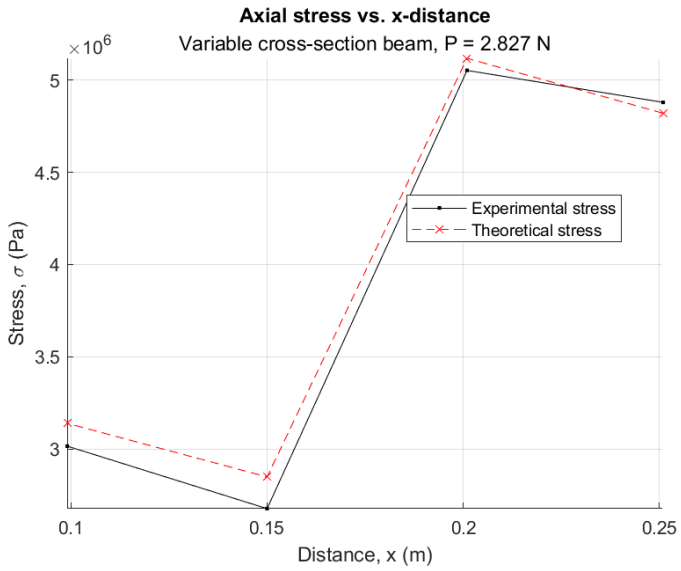

Figure 13: Axial stress over the length of the beam, $P = 2.827\,N$

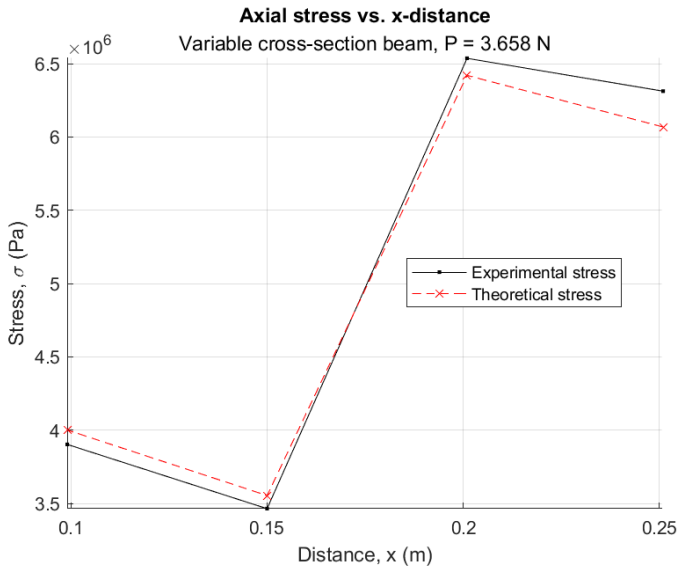

Figure 14: Axial stress over the length of the beam, $P = 3.658\,N$

For the variable cross section beam, there is still good accuracy between computed and collected results. While some outliers, the slopes of each line segment are generally consistent with analytical results, i.e. the theory expected some variation. This is also to note that 'constant stress' was not really seen. Each of the segments with a softer slope, i.e. $\sim 0.9 > x > 0.55$ and $\sim 0.2 < x < 0.26$, are areas where the material thickness gradually increases from the first point to the second point to maintain a constant stress, effectively making up for the longer moment arm by distributing the internal bending forces over a larger area. This is reflected in Eq. [1] equation for bending stress, where the larger cross-section has a larger moment of inertia, which is inversely proportional to stress.

$$\sigma_{axial} = \frac{M(x) \cdot y_{max}}{I(x)} \qquad [1]$$

Holding y_{max} and $M(x)$ constant, as these do not change as a function of the width:

$$y_{max} = \frac{h}{2}; \qquad M(x) = P \cdot x$$

$$\sigma_{axial} \propto \frac{1}{I(x)}$$

Where $I(x)$ is the inertia as a function of the location on the beam, which varies according to width as b by:

$$I(x) = \frac{bh^3}{12}$$

In the plots for each of the magnitudes, the analytically computed stress did not predict that this would be entirely successful, and the experimental data matches this. The discrepancy seen here, since it is seen in both data sets, is likely due to human dimensions measurement error or machine error – likely the former. Relatively speaking along the variable cross-section beam however, the regions intended for constant stress have a much smaller magnitude of derivative compared to the center region, where the geometry changes to setup the next constant stress region. This demonstrates that the change in geometry does have non-negligible effect, and with no measurement errors or a more

carefully designed beam, constant or more ideal stress can be achieved as a function of physical geometry. A second potential source of error is using the computed Young's modulus, as this experimental value is roughly 10% lower than published data. Other sources of error may include uncertainty in strain gauge placement, physical impurities or damages to the test object, assumptions made to derive the analytical equations, or limits of theory in predicting exact stresses.

IV. Conclusion

The bending of Aluminum 7075 cantilever beams was investigated experimentally, and strain measurements were used to determine Young's modulus and Poisson's ratio. The results showed a consistent linear relationship between applied load and strain, confirming the assumptions of elastic bending theory. The stress distribution along the beams with uniform and varying cross-sections followed expected trends, with deviations attributed to strain gage placement, material inconsistencies, and experimental limitations. The constant stress beam demonstrated a smaller stress derivative in the desired constant-stress regions, aligning with theoretical predictions. While some discrepancies were seen between experimental and analytical results, these were within reasonable limits given potential measurement error or simplifying assumptions. The experiment successfully reinforced theoretical concepts seen in lectures and homework with physical experience.

V. Appendix A: MATLAB Code

```
%% Header
% Author: Zakary Steenhoek
% Date: 19 February 2025
% Title: AEE325 Lab02

% Reset
clc; clear;

%% Setup

% Variables (m typ.)
PR_L = 0.26;
PR_W = 0.02544;
PR_T = 0.00631;
DS_L = [0.26 0.184 0.108];
DS_W = 0.02544;
DS_T = 0.00631;
CS_L = [0.251 0.201 0.15 0.099];
CS_W = [0.02171 0.01679 0.02364 0.01385];
CS_T = .00634;
localPath = 'AEE325\Lab-2\figs';
syms F X Y I C1 eA C B H MX YM

% Equations
M = F.*X;
SA1 = (MX.*Y)./(I);
SA2 = C1.*eA;
SA3 = YM.*eA;
P = solve(SA1 == SA2, F);
EP = (C.*Y.*X)./I;
I = 1/12.*(B.*H.^3);

% Functions
moment = matlabFunction(M);
axialStress1 = matlabFunction(SA1);
axialStress2 = matlabFunction(SA2);
axialStress3 = matlabFunction(SA3);
load = matlabFunction(P);
youngsMod = matlabFunction(EP);
rectInertia = matlabFunction(I);

%% Data

% Poissons ratio beam
dataFilePR = importdata(buildPath('AEE325\Lab-2\data\PoissonsRatio.txt'));
PR_F = dataFilePR.data(:,2);
PR_us = dataFilePR.data(:,3:4);

% Distributed stress beam
dataFileDS = importdata(buildPath('AEE325\Lab-2\data\DistStress_data.txt'));
DS_F = dataFileDS.data(:,2);
DS_us = dataFileDS.data(:,3:5);
```

```
% Constant stress beam
dataFileCS = importdata(buildPath('AEE325\Lab-2\data\ConstStress_data.txt'));
CS_F = dataFileCS.data(:,2);
CS_us = dataFileCS.data(:,3:6);

%% Math

% Linear regression of load-strain
loadStrain = polyfit(PR_us(:,1),PR_F,1);

% Coefficient of the load-strain data -> E
C1 = loadStrain(1)*10^6;
PR_I = rectInertia(PR_W,PR_T);
E = youngsMod(C1,PR_I,PR_L,PR_T/2);

% Linear regression of strain-strain
strainStrain = polyfit(PR_us(:,1),PR_us(:,2),1);

% Coefficient of the strain-strain data -> Posson's ratio
C2 = strainStrain(1);
PR_ratio = C2;

% Intertia for both beams
DS_I = rectInertia(DS_W,DS_T);
CS_I = rectInertia(CS_W,CS_T);

% Moments for both beams
DS_M = moment(DS_F,DS_L);
CS_M = moment(CS_F,CS_L);

% Exp axial stress for both beams
DS_S_exp = axialStress1(DS_I,DS_M,DS_T/2);
CS_S_exp = axialStress1(CS_I,CS_M,CS_T/2);

% Analytical axial stress for both beams
DS_S_ana = axialStress3(E,DS_us.*10^-6);
CS_S_ana = axialStress3(E,CS_us.*10^-6);


%% Plots

% Diagrams for constant cross section beam
simpcantSM(max(DS_L), max(DS_F),max(DS_L),{'m', 'N'},1);
% autosave('shear-moment', localPath, 1);

% Load-strain plot
figure(1); clf; hold on; grid on;
title('Load-strain diagram')
xlabel('Axial microstrain, \epsilon*10^{-6}'); ylabel('Load, P (N)');
plot(PR_us(:,1),PR_F,'rx')
fplot(poly2sym(loadStrain),'k-')
legend('Force-strain data', 'Regression curve', Location='best');
xlim([min(PR_us(:,1)) max(PR_us(:,1))]); ylim([min(PR_F) max(PR_F)]);
hold off;
% autosave('load-strain', localPath);
```

```
% Strain-strain plot
figure(2); clf; hold on; grid on;
title('Strain-strain diagram')
xlabel('Axial microstrain, \epsilon*10^{-6}');
ylabel('Transverse microstrain, \epsilon*10^{-6}');
plot(PR_us(:,1),PR_us(:,2),'rx')
fplot(poly2sym(strainStrain),'k-')
legend('Strain-strain data', 'Regression curve', Location='best');
xlim([min(PR_us(:,1)) max(PR_us(:,1))]);
ylim([min(PR_us(:,2)) max(PR_us(:,2))]);
hold off;
% autosave('strain-strain', localPath);

% Distributed stress plots
figure(31); clf; hold on; grid on;
subtitle = 'Constant cross-section beam, P = ' + string(DS_F(1)) + ' N';
title('Axial stress vs. x-distance', subtitle)
xlabel('Distance, x (m)'); ylabel('Stress, \sigma (Pa)');
plot(DS_L, DS_S_exp(1,:),'k.-')
plot(DS_L, DS_S_ana(1,:),'rx--')
legend('Experimental stress', 'Theoretical stress', Location='best');
xlim([min(DS_L) max(DS_L)]);
ylim([min(DS_S_ana(1,:)) max(DS_S_exp(1,:))]);
hold off;

figure(32); clf; hold on; grid on;
subtitle = 'Constant cross-section beam, P = ' + string(DS_F(2)) + ' N';
title('Axial stress vs. x-distance', subtitle)
xlabel('Distance, x (m)'); ylabel('Stress, \sigma (Pa)');
plot(DS_L, DS_S_exp(2,:),'k.-')
plot(DS_L, DS_S_ana(2,:),'rx--')
legend('Experimental stress', 'Theoretical stress', Location='best');
xlim([min(DS_L) max(DS_L)]);
ylim([min(DS_S_ana(2,:)) max(DS_S_exp(2,:))]);
hold off;

figure(33); clf; hold on; grid on;
subtitle = 'Constant cross-section beam, P = ' + string(DS_F(3)) + ' N';
title('Axial stress vs. x-distance', subtitle)
xlabel('Distance, x (m)'); ylabel('Stress, \sigma (Pa)');
plot(DS_L, DS_S_exp(3,:),'k.-')
plot(DS_L, DS_S_ana(3,:),'rx--')
legend('Experimental stress', 'Theoretical stress', Location='best');
xlim([min(DS_L) max(DS_L)]);
ylim([min(DS_S_ana(3,:)) max(DS_S_exp(3,:))]);
hold off;

figure(34); clf; hold on; grid on;
subtitle = 'Constant cross-section beam, P = ' + string(DS_F(4)) + ' N';
title('Axial stress vs. x-distance', subtitle)
xlabel('Distance, x (m)'); ylabel('Stress, \sigma (Pa)');
plot(DS_L, DS_S_exp(4,:),'k.-')
plot(DS_L, DS_S_ana(4,:),'rx--')
legend('Experimental stress', 'Theoretical stress', Location='best');
xlim([min(DS_L) max(DS_L)]);
ylim([min(DS_S_ana(4,:)) max(DS_S_exp(4,:))]);
```

```
hold off;

figure(35); clf; hold on; grid on;
subtitle = 'Constant cross-section beam, P = ' + string(DS_F(5)) + ' N';
title('Axial stress vs. x-distance', subtitle)
xlabel('Distance, x (m)'); ylabel('Stress, \sigma (Pa)');
plot(DS_L, DS_S_exp(5,:),'k.-')
plot(DS_L, DS_S_ana(5,:),'rx--')
legend('Experimental stress', 'Theoretical stress', Location='best');
xlim([min(DS_L) max(DS_L)]);
ylim([min(DS_S_ana(5,:)) max(DS_S_exp(5,:))]);
hold off;
% autosave('DistStress', localPath, 1);

% Constant stress plots
figure(41); clf; hold on; grid on;
subtitle = 'Variable cross-section beam, P = ' + string(CS_F(1)) + ' N';
title('Axial stress vs. x-distance', subtitle)
xlabel('Distance, x (m)'); ylabel('Stress, \sigma (Pa)');
plot(CS_L, CS_S_exp(1,:),'k.-')
plot(CS_L, CS_S_ana(1,:),'rx--')
legend('Experimental stress', 'Theoretical stress', Location='best');
xlim([min(CS_L) max(CS_L)]);
ylim([min(CS_S_exp(1,:)) max(CS_S_ana(1,:))]);
hold off;

figure(42); clf; hold on; grid on;
subtitle = 'Variable cross-section beam, P = ' + string(CS_F(2)) + ' N';
title('Axial stress vs. x-distance', subtitle)
xlabel('Distance, x (m)'); ylabel('Stress, \sigma (Pa)');
plot(CS_L, CS_S_exp(2,:),'k.-')
plot(CS_L, CS_S_ana(2,:),'rx--')
legend('Experimental stress', 'Theoretical stress', Location='best');
xlim([min(CS_L) max(CS_L)]);
ylim([min(CS_S_exp(2,:)) max(CS_S_ana(2,:))]);
hold off;

figure(43); clf; hold on; grid on;
subtitle = 'Variable cross-section beam, P = ' + string(CS_F(3)) + ' N';
title('Axial stress vs. x-distance', subtitle)
xlabel('Distance, x (m)'); ylabel('Stress, \sigma (Pa)');
plot(CS_L, CS_S_exp(3,:),'k.-')
plot(CS_L, CS_S_ana(3,:),'rx--')
legend('Experimental stress', 'Theoretical stress', Location='best');
xlim([min(CS_L) max(CS_L)]);
ylim([min(CS_S_exp(3,:)) max(CS_S_ana(3,:))]);
hold off;

figure(44); clf; hold on; grid on;
subtitle = 'Variable cross-section beam, P = ' + string(CS_F(4)) + ' N';
title('Axial stress vs. x-distance', subtitle)
xlabel('Distance, x (m)'); ylabel('Stress, \sigma (Pa)');
plot(CS_L, CS_S_exp(4,:),'k.-')
plot(CS_L, CS_S_ana(4,:),'rx--')
legend('Experimental stress', 'Theoretical stress', Location='best');
xlim([min(CS_L) max(CS_L)]);
```

```
ylim([min(CS_S_exp(4,:)) max(CS_S_ana(4,:))]);
hold off;

figure(45); clf; hold on; grid on;
subtitle = 'Variable cross-section beam, P = ' + string(CS_F(5)) + ' N';
title('Axial stress vs. x-distance', subtitle)
xlabel('Distance, x (m)'); ylabel('Stress, \sigma (Pa)');
plot(CS_L, CS_S_exp(5,:),'k.-')
plot(CS_L, CS_S_ana(5,:),'rx--')
legend('Experimental stress', 'Theoretical stress', Location='best');
xlim([min(CS_L) max(CS_L)]);
ylim([min(CS_S_exp(5,:)) max(CS_S_exp(5,:))]);
hold off;
% autosave('ConstStress', localPath, 1);
```

VI.References

[1] MatWeb. *Aluminum 7075-T6 Mechanical Properties*. Available: https://www.matweb.com/search/datasheet.aspx?MatGUID=4f19a42be94546b686bbf43f79c51b7d. Accessed: Feb. 19, 2025.

[2] MakeItFrom. *7075-T6 Aluminum Material Properties*. Available: https://www.makeitfrom.com/material-properties/7075-T6-Aluminum. Accessed: Feb. 19, 2025.

[5*] MathWorks. *MATLAB Central - Answers*. Retrieved from https://www.mathworks.com/matlabcentral/answers/index/?s_tid=gn_mlc_an.

[6*] MathWorks. *MATLAB Documentation - Help Center*. Retrieved from https://www.mathworks.com/help/index.html?s_tid=CRUX_lftnav.

[7] Arizona State University. (2025). *Lab 2 - Bending of Cantilever Beams*. Retrieved from AEE325 Canvas

[8] Arizona State University. (2025). *Lab 2 - Bending of Cantilever Beams – Procedure and Checklist*. Retrieved from AEE325 Canvas

[9] Arizona State University. Unpublished data. Retrieved from AEE325 Canvas

*: Denotes ‘main page’ sources, from which numerous specific pages were visited.